Fish and Shellfish Immunology 95 (2019) 220–226

Contents lists available at ScienceDirect

Fish and Shellfish Immunology

journal homepage: www.elsevier.com/locate/fsi

Full length article

cGAMP inhibits tumor growth in colorectal cancer metastasis through the STING/STAT3 axis in a zebrafish xenograft model

Xiaofeng Jiang[a,b,1,*], Guangping Liu[c], Zhiyi Hu[a,b], Guiqian Chen[a,b], Jianqing Chen[a,b], Zhengbing Lv[a,b,**,1]

[a] College of Lifescience and Medicine, Zhejiang Sci-Tech University, Hangzhou, 310018, China
[b] Zhejiang Provincial Key Laboratory of Silkworm Bioreactor and Biomedicine, Hangzhou, 310018, China
[c] College of Life Sciences, Yan'an University, Yan'an, 716000, China

ARTICLE INFO

Keywords:
cGAMP
Colorectal cancer
STING/STAT3 axis
Metastasis

ABSTRACT

The leading cause of mortality due to colorectal cancer (CRC) is highly associated with the development of liver metastases. Recently, we described cGAMP that is closely related to the metastatic state wherein the progress of metastatic tumors is associated with favorable outcomes in a zebrafish xenograft model. cGAMP was administered and the expression levels of type-I interferons were induced amongst tumor tissues to illuminate the overall measure of the induced STING/STAT3 axis in colorectal liver metastases. Furthermore, cGAMP–STING dependent STAT3 activation resulted in the inhibition of tumor cell proliferation, viability, and invasion in vitro. The subtotal reduction in tumor growth attributed to a large number of infiltrating inflammatory cells in vivo. We showed that cGAMP inhibited migration through angiogenesis by up-regulating IL-2, TNF-α, and IFN-γ, whereas STAT3 down-regulation inhibited CXCL8, BCL-2, and VEGFA expression. The importance of cGAMP in inhibiting the invasion front of CRC confirmed that the cGAMP dependent activation of STING/STAT3 axis played a key role in the inhibition of tumor progression.

1. Introduction

Liver is the most common metastatic site of colorectal cancer (CRC), and liver metastasis is found in almost 40% of the patients who died of CRC [1]. There were estimated a 5-year survival rate of 20%–40% in patients with CRC and confined liver metastasis, therefore, liver metastasis is the leading cause of death of the patients with advanced CRC [2]. Liver metastases are commonly inoperable and are associated with poor prognosis [3]. Diagnosis of liver metastasis is a serious issue that must be considered in CRC clinical treatment. Developing of new agents for reducing the risk of liver metastasis in high-risk groups of patients and establishing prognostic markers of recurrence following liver resection are extremely important [4].

The mechanisms that drive antitumor immune responses to tumor metastasis remain poorly understood. The certain cytokines in the tumor microenvironment (TME) have a pivotal role in liver metastasis [5–7]. Previous studies indicated that CXCL8 (chemokine ligand 8, also called IL-8), a key member of the ELR (+) CXC chemokine family, and plays an important role in CRC liver metastasis due to its angiogenic effect [8]. Although the importance of CXCL8 and its receptor in CRC liver metastasis has been illuminated, the concrete mechanism of induced or inhibitory pathway of regulating of CXCL8 expression in the process of tumor cells homing to liver remains unkown. Further research on the cross-talk between tumor cells and the invasion front and the regulation of cytokines during tumor development, progression, and proliferation would provide further insights into disease progression and resistance to existing therapies and help develop novel antitumor agents [9,10]. Specific spontaneous STING activation is required for the spontaneous induction of antitumor immunity [11]. STING is activated through tumor DNA-dependent activation of cGAS and the generation of endogenous cGAMP; moreover, other cyclic nucleotides, such as cGAMP and c-di-AMP, are also exogenous STING ligands that activate type-I IFN expression [11–13]. However, the cellular mechanism underlying this response and whether this mechanism could enhance the generation of antitumor immune responses should be further studied. Whether the agonist-mediated activation of STING could inhibit tumor

* Corresponding author. College of Lifescience And Medicine, Zhejiang Sci-Tech University, Hangzhou 310018, China.
** Corresponding author. College of Lifescience And Medicine, Zhejiang Sci-Tech University, Hangzhou, 310018, China.
E-mail addresses: xfjiang@zstu.edu.cn (X. Jiang), liugp0093@aliyun.com (G. Liu), hu.zhiyi@foxmail.com (Z. Hu), gqchen@zstu.edu.cn (G. Chen), cjqgqj@126.com (J. Chen), zhengbingl@zstu.edu.cn (Z. Lv).
[1] The co-corresponding authors

https://doi.org/10.1016/j.fsi.2019.09.075
Received 25 June 2019; Received in revised form 28 September 2019; Accepted 30 September 2019
Available online 02 October 2019
1050-4648/

progression and metastasis via the STING/STAT3 axis through the down-regulation of CXCL8 remains unknown.

Here, the zebrafish xenograft model was used to evaluate the inhibition ability of STING/STAT3 axis in tumor angiogenesis of MC38 colorectal cancer cells. We focused on cGAMP to understand its role in the host–tumor interaction site. CXCL8 and VEGFA that were down-regulated by cGAMP via the STING/STAT3 axis in tumor tissue inhibited CRC metastasis. The shRNA-mediated knockdown of STING or STAT3 in MC38 cells also drastically reduced cell proliferation, migration, and invasion in vitro and resulted in the subtotal reduction of tumor growth in vivo. Our work and previous studies indicated that cGAMP may serve as a potential target in the treatment of CRC liver metastasis.

2. Results

2.1. shRNA-mediated knockdown of STING and STAT3 reduces mRNA and protein levels in MC38 cells

The expression levels of *Tmem173* and *STAT3* genes in MC38 cells were knockdown respectively by using shRNA silencing method to evaluate the role of endogenous STING-STAT3 axis in tumor invasion and metastasis. Real-time quantitative PCR (Q-PCR) and Western blot analyses were used for evaluate the ability of shRNAs to silence the expression of target genes in vitro. The Q-PCR results revealed that the Tmem173 mRNA level was down-regulated to 20% (Fig. 1A). The Western blot analysis revealed that the activated STING and STAT3 protein levels decreased to 6% and 10%, respectively (Fig. 1B). The clear target bands with the expected molecular weight of STING and STAT3 were detected in Supplementary data (Fig. S1). The Tmem173 mRNA or STING and STAT3 protein levels in MC38 cells transfected with nonspecific shRNA (shNTC) did not significantly differ from those in MC38 cells.

2.2. Intratumoral cGAMP injection promotes Th1 cytokine induction, reduces CXCL8/VEGFA expression, and inhibits tumor growth

We established a zebrafish xenograft CRC model to evaluate the STING-dependent induction of the host antitumor immunity. MC38 cells and cGAMP or cGAMP were intraperitoneally injected into wild-type (WT) AB strain or STING-deficient ($STING^{gt/gt}$) zebrafish. Changes in some certain Th1 cytokines, CXCL8, VEGFA, TGF-β, MET and HGF expression levels and the tumor size were quantified. The results showed considerably induced expression of IL-2, TNF-α, and IFN-γ, and accelerated tumour growth in $STING^{gt/gt}$ zebrafish relative to those in WT zebrafish (Fig. 2A and B). The antitumor efficacy of cGAMP was further enhanced by the down-regulation of CXCL8 and VEGFA (Fig. 2 C) in a STING-dependent manner. The inductive effects of CXCL8 and VEGFA shows that the inhibitory effect of cGAMP (2′-5′, 3′-5′) was stronger than that of c-di-GMP. These data indicated that the activation of STING enforced by intratumoral cGAMP injection can efficiently control tumor growth by up-regulating Th1 cytokine expression and reducing CXCL8 and VEGFA expression. A large proportion of CRC metastases display activation of the TGF-β pathway and they are characterized by elevated TGF-β production. In our study, not surprisingly, after administrated cGAMP to all groups of zebrafish, the observation that the expression of TGF-β, MET and HGF in STING deficient zebrafish were dramatically elevated than those in the WT fish after MC38 cells transplantation (Fig. 2 D & E). In addition, we observed that the well-characterized direct transcriptional gene targets of TGF-β, such as *PAI-1*, *SMAD7* and *CTGF* (Fig. S2), were more expressed in STING-deficient zebrafish embryonic fibroblast cells than WT fish group after MC38 cells had been transplanted. These data suggest that STING may play an antitumorigenic role in CRC.

2.3. STAT3 knockdown accelerates cell proliferation and enhances cell viability

We performed cell counting, Annexin-V and CCK-8 assays to examine the effect of silencing STAT3 before cGAMP injection on cell proliferation and viability. As shown in Fig. 3A and B, the proliferation and viability of shSTAT3-transfected cells were moderately enhanced relative to those of shNTC and control MC38 cells. STAT3 silencing significantly reduced the IFN-1 and IL-12 expression but up-regulated the IL-4 and IL-10 expression (Fig. 3 C). The results of the flow cytometry and the CCK-8 assays indicated that the apoptotic status and dead cells of the cGAMP stimulated shSTAT3 group significantly differed from the control cells (Fig. 3 D). Meanwhile, the in vivo detection of the tumor infiltrated NKT-like phenotype cells showed a remarkable increase in cGAMP induced WT fish compared with STAT3-deficient zebrafish (Fig. 3 E).

2.4. Inhibiting STING and STAT3 activation attenuates tumor invasion in vitro and metastasis in vivo

We tested the invasive capacity of MC38 cells by using Matrigel invasion chambers (Fig. 4). The invasive capacity of tumor cells was dramatically affected. The invasive capacity of MC38 cells injected with cGAMP decreased by 15-fold relative to that of control cells, and STING inhibition almost removed the anti-invasion capacity of the cells (Figure 4A). Interestingly, STING inactivation resulted in low STAT3 activation, and the invasive capacity of tumor cells with normal STING levels but deficient activated STAT3 levels was enhanced relative to that of shNTC cells (Figure 4A). Tumor-transplanted zebrafish received intraperitoneal injections of cGAMP followed by injections of shSTING, shSTAT3, and shNTC MC38 cells. Metastasis to the liver was monitored over a 6–8 week period to determine whether the tumorigenic potential of MC38 cells in vivo would be affected by the downregulation of the STING/STAT3 axis in conjunction with cGAMP injection. ShNTC cells produced small tumors, whereas shSTING and shSTAT3 clones

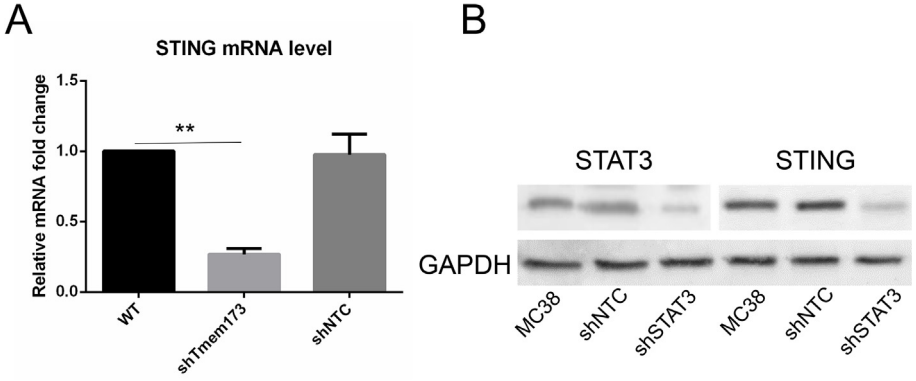

Fig. 1. Down-regulation of STING and STAT3 expression in MC38 cells by shRNA. Cells were transfected with the appropriate shRNA plasmids as described in the Materials and Methods section. Q-PCR (A) was performed to analyze the expression of STING mRNA after the selection of stable cell lines. Comparing the Western blots (B) of extracts from MC38 cells that had been stably transfected with shSTING and shSTAT3 with those of extracts from shNTC and control MC38 cells showed that STING and STAT3 had been down-regulated. All data are representative of at least three independent experiments. **p < 0.01. The full-length blots/figure source files are presented in Supplementary Fig. S1.

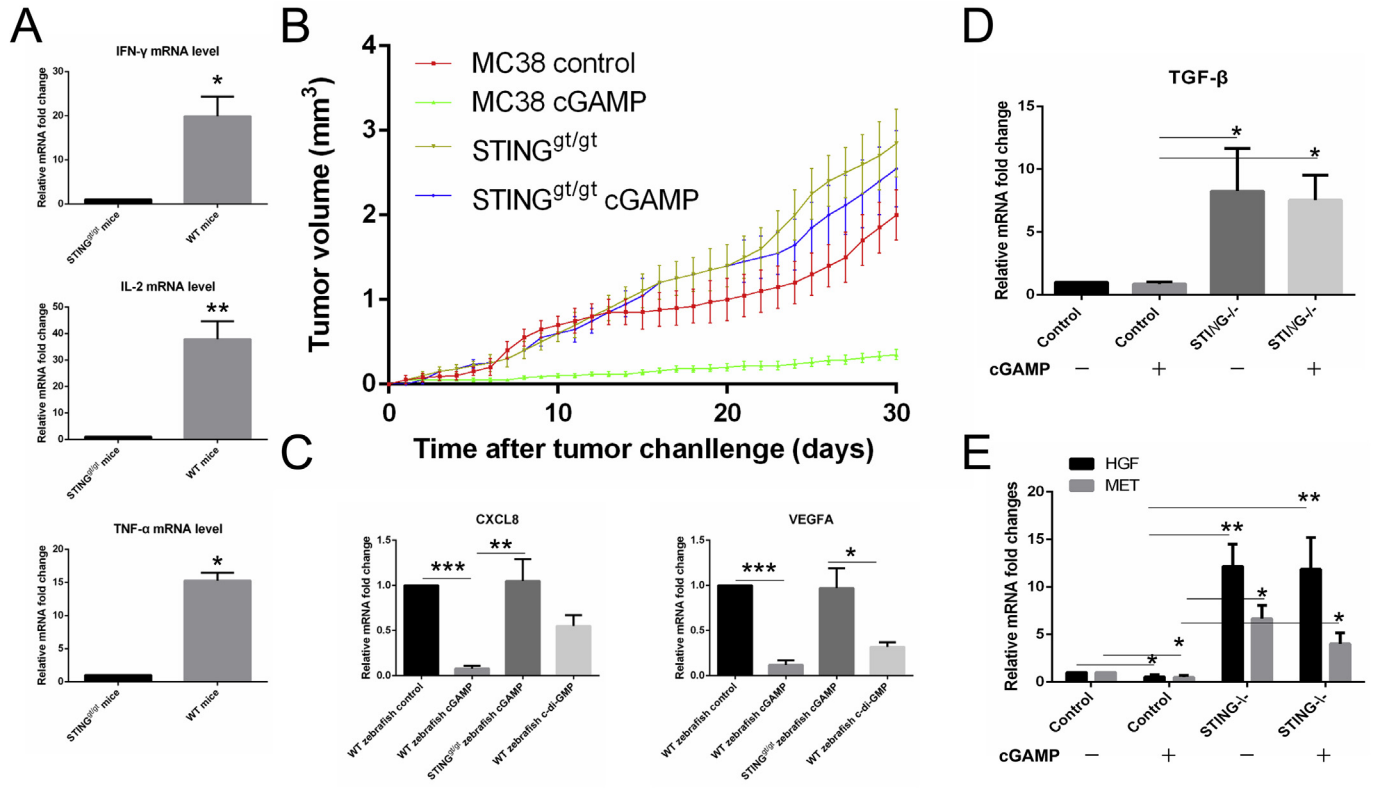

Fig. 2. cGAMP suppresses tumors by promoting Th1 response and reducing CXCL8/VEGFA expression. QPCR revealed that cGAMP induced the expression of the Th1 cytokines IFN-γ, IL-2, and TNF-α (A). cGAMP was administered intratumorally to WT and STING$^{gt/gt}$ zebrafish. Tumor growth was monitored from day 0 to day 30 after cGAMP injection (B). QPCR analysis revealed that cGAMP mediated CXCL8 and VEGFA down-regulation (C). QPCR detections of the mRNA changes of TGF-β (D), HGF and MET (E), cGAMP(+) represents intraperitoneal administered of 1 μg of cGAMP per fish, cGAMP(−) represents intraperitoneal administered PBS. All data are representative of at least three independent experiments. *p < 0.05, **p < 0.01, ***p < 0.001.

demonstrated enhanced tumorigenic potential (Figure 4B). Furthermore, the expression levels of proangiogenic VEGFA and antiapoptotic BCL-2 mRNA levels in cells with shRNA-mediated STAT3 knockdown decreased relative to that in WT MC38 cells (Figure 4C) after cGAMP stimulation. The cGAMP-induced STAT3-dependent inhibition of Bcl-2 would largely suppress the growth of MC38 cells. The tissue immunohistochemistry results demonstrated that positive VEGFA staining in STING$^{gt/gt}$ zebrafish intensified ($p < 0.01$, Figure 4D) relative to that in WT zebrafish after cGAMP induction. These data collectively indicate that the cGAMP–STING/STAT3 axis may activate proangiogenic and antiapoptotic pathways, and cGAMP is a potential anti-metastasis agent.

3. Discussion

Our study demonstrates that the intratumoral injection of cGAMP induces potent STING–STAT3 activation in the TME and thereby inhibits tumor growth by promoting Th1 immune responses and inhibiting antitumor VEGFA and BCL-2 expression. Efficient vaccines against intracellular pathogens or cancer require adjuvants that induce type-1 immune responses [14]. Cyclic dinucleotides, such as cGAMP and c-di-GMP, have attracted attention as potential vaccine adjuvants because they directly bind to the transmembrane molecule STING and activate the TBK1–IRF3–dependent signalling pathway to induce type-I IFNs [15,16].

The intratumoral injection of cGAMP induced CXCL8 expression via the STING/STAT3 axis and the subsequent decline in VEGFA and BCL-2 (Fig. 2). The STING/STAT3 axis mediated induction of type I IFNs and the tumor infiltrated NKT-like phenotype cells. Chemokines are small (6–14 kDa) secreted proteins with four different classes: CC, XC, CXC, and CX3C [17]. CXCL8 belongs to the CXC class of chemokines and is associated with inflammation and immune response; moreover, it is also an important biomarker for several diseases, including different cancer types, and promotes CRC liver metastasis [18]. Our results indicate that cGAMP administration would enhance antitumor immunity through the STING/STAT3 axis. Proinflammatory factors, such as e IL-2, TNF-α, and IFN-γ, were significantly induced and tumor growth declined in WT zebrafish relative to those in STING$^{gt/gt}$ zebrafish (Fig. 2A and B). CXCL8 inhibition by cGAMP was also strictly dependent on the STING/STAT3 axis and resulted in VEGFA and BCL-2 down-regulation. The continued growth of tumor cells was dependent on the development of an intact tumor vasculature. Vascular endothelial growth factor and BCL-2 participate in the promotion of tumor angiogenesis and homeostasis [19–21]. The down-regulation of CXCL8 through the cGAMP–STING–STAT3 pathway inhibits tumor growth in CRC liver metastasis. Intratumoral STING activation by cGAMP and other potential ligands is an attractive candidate for the antitumor therapy of patients with CRC. Given that the efficacy of intratumoral cGAMP is strongly enhanced by the up-regulation of Th1 responses and the down-regulation of VEGFA, STING agonists are potential immunotherapeutic agents in CRC liver metastasis [22]. As a key molecular in cell proliferation and metastasis, the *MET* oncogene encodes for the Met tyrosine kinase receptor for HGF, MET could be activated by the induction of HGF and then strengthen the tumor cell survival and metastasis through PI3K-AKT-mTOR and RAS-RAF-MEK-ERK pathways [23,24]. Our preliminary appraisal of MET and HGF copy number variations in normal and STING-deficiency zebrafish revealed that the focal amplification of these genes in tumor tissue may largely depend on the absence of STING. The TGF-β pathway was also activated by knockout STING, thus makes the cGAMP-STING/STAT3 axis a potential key node in CRC proliferation and metastasis.

Zebrafish tumor xenografts model is considered a novel research

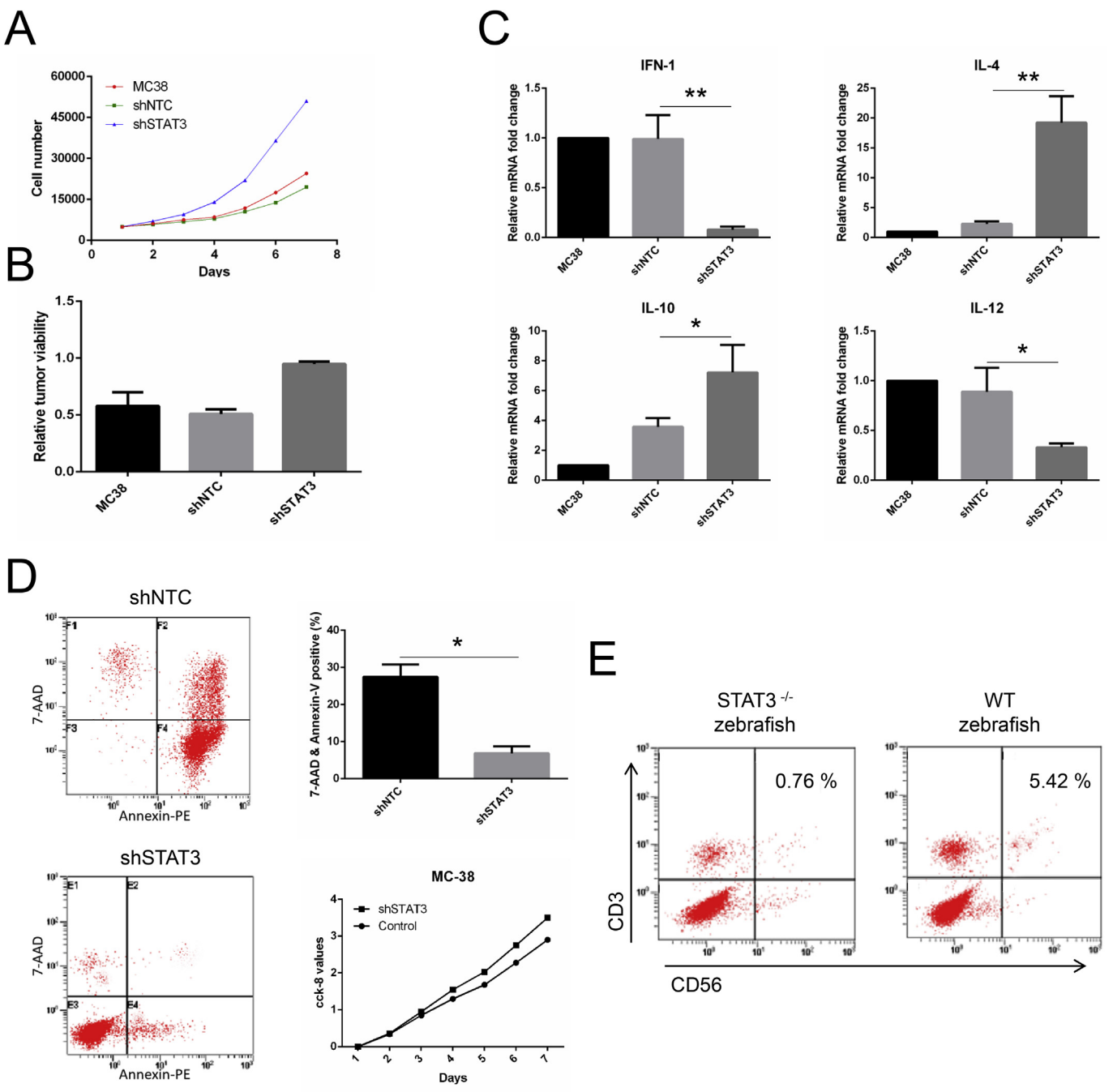

Fig. 3. Knockdown of STAT3 promotes tumor proliferation and viability in vitro. Cell counting (A) revealed that the proliferation of STAT3 knockdown cells drastically increased relative to that of shNTC and control MC38 cells. MTT assay (B) showed that the viability of STAT3 knockdown cells was enhanced relative to that of shNTC and control cells. Q-PCR analysis (C) was performed to detect steady-state IFN-β, IL-12, IL-4, and IL-10 mRNA levels. 7-ADD and Annexin-V positive staining results and CCK-8 assays result (D) for detecting apoptosis and necrosis of cells lacking expression of STAT3 or vector control under cGAMP stimulation. The changes of NKT-like cells between groups were detected by the flow cytometry (E). All data are representative of at least three independent experiments. *$p < 0.05$, **$p < 0.01$.

model for evaluating the effects of the new antitumor therapies or antineoplastic drugs [25]. The model is widely used in the early screening of antineoplastic drugs and therapies [26,27]. However, few works have used the model to study the tumor immnuotherapy on CRC metastasis is still lacking. Our study primitively used the zebrafish as the MC38 tumor cell transplantation model to evaluate the inhibitory effects of STING/STAT3 dependent cGAMP on CRC metastasis. This research also explored ways to develop the zebrafish xenograft model that can accurately test the effect of immunotherapies against tumors to improve the research and development of novel anticancer therapies.

Our research also identified the key role of the vasculature of growing tumors in shaping cGAMP-mediated STING/STAT3-dependent antitumor immunity (Fig. 4). This finding raises questions about the effects of antiangiogenic therapies [28] that are being developed as novel antitumor agents for the treatment of CRC liver metastasis.

In conclusion, our study provides important evidence that CXCL8 and VEGFA down-regulation induced by cGAMP-mediated STING/STAT3-dependent antitumor immunity at the tumour invasion front in a zebrafish CRC xenograft model contributes to the inhibition of colon cancer cell proliferation, migration, invasion and angiogenesis. These

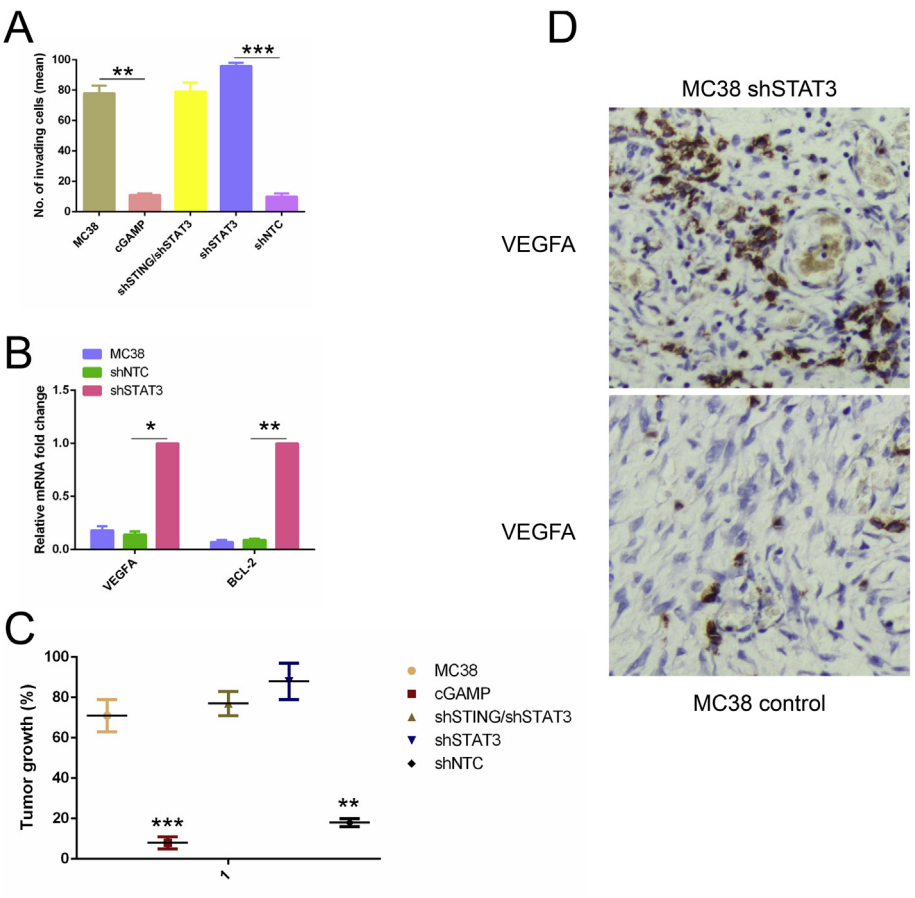

Fig. 4. STING and STAT3 knockdown in MC38 cells abrogates tumor growth in vivo. The numbers of cGAMP-induced cells that transmigrated across Matrigel chambers were lower that those of shSTING and shSTAT3 cells (A). cGAMP-induced cells (n = 10), cGAMP-induced shSTING/shSTAT3 (n = 10), cGAMP-induced shSTAT3 (n = 10), cGAMP-induced shNTC (n = 10), or control MC38 (n = 12) cells were intraperitoneal injected into the different groups of zebrafish, and the tumor growth was determined after the zebrafish were sacrificed. Similar to MC38 cells, shSTING and shSTAT3 or shSTAT3 cells produced large tumors. By contrast, cGAMP-induced shNTC clones have lost their tumorigenic potential (B). VEGFA and BCL2 expression levels in STAT3 knockdown cells were higher than those in shNTC and control cells (C). VEGFA expression was detected through the immunohistochemical analysis of tissue microarrays (D). Representative images of VEGFA expression in WT (Above) and STING$^{gt/gt}$ zebrafish (Below). The inset shows an image that was acquired under 200 × magnification. All data are representative of at least three independent experiments. *p < 0.05, **p < 0.01, ***p < 0.001.

findings may provide basis to support the development of novel STING agonist therapies for CRC treatment.

4. Material and methods

4.1. Cell lines and animal experiments

The primary zebrafish embryonic fibroblast cells and MC38 cells were cultured in RPMI medium supplemented with 10% FCS, 2 mM glutamine, 100 IU/ml penicillin and 50 mg/ml streptomycin. Tumor metastasis was induced in the wild-type (WT) AB strain zebrafish, *Tmem173*$^{-/-}$ and *STAT3*$^{-/-}$ zebrafish (Kindly provided by Dr. Zhong Liang from Zhejiang University, China) with intraspleenic injection of 4 × 10^6 cells. All experiments were combined injection of 10 μg of 2′5′-3′5′ cGAMP (or 10 μg of c-di-GMP) as mentioned in the results section. After extensive colonization of tumors in the liver (6–8 weeks), the animals were euthanized, livers were removed and the tumor growth rate was measured. All the zebrafish were maintained under specific pathogen free conditions and used in accordance to the animal experimental guidelines set by the Institute of Animal Care and Use Committee. This study has been approved by the Institutional Animal Care and Use Committee of the Zhejiang Sci-Tech University.

4.2. Real time quantitative PCR

Reverse transcription, qPCR normalization and efficiency correction on β-actin RNA were performed as described in our earlier publication [29]. Primers for qPCR assays were purchased from Sangon (Shanghai, China). Primer sequences are listed in Supplementary data (Table S1).

4.3. ShRNA transfection for silencing target genes

MC38 cells were transfected with two different pSM2C plasmids containing Tmem173 shRNAmir constructs (shTmem173) and STAT3 shRNAmir constructs (shSTAT3) from Open Biosystems USA or non-silencing shRNAmir construct (shNTC) according to the manufacturer's instructions. Briefly, 2 × 10^5 MC38 cells were seeded in 6-well plates and subsequently transfected using 10 ml Arrestin™ transfection reagent containing 4 mg indicated shRNAmir. After 6 h incubation, medium was replaced by standard culture medium and stable clones were selected by adding 2 mg/ml puromycin after 48 h.

4.4. Western blots

The rabbit anti-STING and anti-STAT3 polyclonal Abs were produced in our labaratory, the anti-GAPDH polyclonal antibody was purchased from Sangon (Shanghai, China). STING, STAT3, CXCL8 as well as the reference protein (GAPDH) sample was separated by 12% SDS-PAGE and transferred onto 0.45-μm polyvinylidene difluoride membranes (Bio-Rad Laboratories) for 90 min at 350 mA, and then blocked with TBST buffer (50 mM Tris-HCl, 150 mM NaCl and 0.1% Tween-20, pH 7.4) containing 5% non-fat dry milk (w/v) at 4 °C overnight. After washing with TBST three times for 30min, the blots were incubated with rabbit anti-phospho-STING Ab (1:1000), rabbit anti-phospho-STAT3 Ab (1:1000), rabbit anti-CXCL8 Ab (1:1000) or rabbit anti-GAPDH Ab (Abcam. 1:3000). The blots were washed thrice with TBST for 30min, and then incubated for 1 h with the HRP-conjugated goat anti-rabbit IgG Ab (Abcam) at room temperature. After washing with TBST, the immunoreactive proteins were visualized using a chemical luminescent immunodetection system (Tanon 4500, Tanon Technology Company). The specificity of Abs was examined by Western blot analysis. The clear target bands with the expected molecular

weight of target genes were detected in every samples examined (Supplementary data Fig. S1). Results indicated that the Abs prepared in our laboratory were highly active and specific.

4.5. Cell proliferation

Proliferation was measured by plating 5×10^3 cells/well in a 12-well plate in complete growth media and cell numbers were counted daily for 6 days by using a haemocytometer following trypsinization. All the experiments were in triplicates and repeated twice.

4.6. Cell viability

Cell viability was determined using MTT assay (Sigma-Aldrich). Briefly, 5×10^3 cells/well were seeded with 200 ml culture medium in 96-well microplates and incubated at 37 °C for 96 h. Then the cells were incubated with complete medium containing 0.5 mg/ml MTT at 37 °C for 2 h. The reduced MTT crystals were dissolved in 100 mL of DMSO/ethanol solution (1:2, Sigma-Aldrich) after removing the MTT solution and the optical densities were measured at 570 nm. The experiments were carried out in triplicate and repeated twice.

4.7. Flow cytometric analysis

The tumor infiltrated NKT like cells in vivo as well as the 7-ADD/Annexin-V positive staining results for detecting apoptosis and necrosis of cells cells were analyzed by flow cytometry. The cells were stained for 30 min on ice with following fluorescence-labeled antibodies (1 μg/2×10^6 cells) purchased from Abcam: anti-mouse CD3-FITC; anti-mouse CD56-CY3. Apoptosis detection was referred to the product manuals (Annexin V Apoptosis Detection Kit, BBI, China). The cells were washed twice with cold PBS and then were analyzed on BD Accuri C6. The data analysis was performed using BD Accuri C6 software (BD Biosciences, US). The CCK-8 assay was performed using Acmec CCK-8 Cell Proliferation and Cytotoxicity Assay Kit (Acmec, China), the cell proliferation detection was referred to the manufacture's instruction.

4.8. Immunohistochemistry

The expression of VEGFA in CRC tissue microarrays was analyzed using rabbit anti-VEGFA Ab (Abcam, 1:3000). Standard immunohistochemical procedures were implemented as follows: The samples on slides embedded with paraffin and formalin were firstly dewaxed in xylene and rehydrated in alcohol gradients of 100, 95, 85 and 75%. The slides were then heated to 95 °C for 30 min to retrieve antigens in the tissues. The activity of endogenous peroxidase was blocked by employing 3% hydrogen peroxide for 10 min. Part of the tissue was covered with normal serum at room temperature for 30 min. Then, the samples on the slides were incubated with antibodies against VEGFA overnight at 4 °C. The slides were subsequently incubated with peroxidase-conjugated AffiniPure goat anti-rabbit (Abcam. 1:500) for 1 h at room temperature. Next, the samples were stained with 3,3′-diaminobenzidine and counterstained with hematoxylin. The procedure of dehydration was implemented, and finally covers slips were applied.

4.9. Matrigel invasion assay

Invasion assays were performed using a standardized Matrigel invasion chamber (8-mm pore size; BD Biosciences, Germany) according to the manufacturer's instructions. Briefly control MC38, shNTC MC38 or target genes silencing MC38 cells in RPMI medium containing 1% FBS (5×10^4 cells/ml) were seeded into the rehydrated matrigel membrane. 750 ml of RPMI (10% FBS) was added into the lower chamber and incubated for 48 h. Non-invading cells from the upper surface of the membrane were removed with a cottontipped swab, fixed for 20 min in ice-cold methanol and invading cells were stained with 1% toluidine blue. To calculate the total number of invading cells, the cell number in the complete membrane cut out (membrane surface area 0.3 cm^2) was counted. The assay was performed in triplicate and repeated twice.

4.10. Data analysis and software

All experiments were repeated at least three times. The statistical evaluations of the differences between the means of the experimental groups were performed using Student's *t*-test, and the data were expressed as the mean ± SD. The criteria for statistical significance used were $^*p < 0.05$, $^{**}p < 0.01$, and $^{***}p < 0.001$ (GraphPad Prism 6.0). The overall survivals rates were presented as Kaplan-Meier estimates and analyzed using the Breslow test. A P value of < 0.05 was considered indicative of statistical significance. The data were analyzed with SPSS statistical software (version 19.0 for Windows, SPSS).

Availability of data and materials

Please contact author for data requests.

Funding

This work was supported by the Start-up of research fund of Zhejiang Sci-Tech University (ZSTU), China, grant No. is 116129A4Y17186.

Authors' contributions

X.F.J. and Z.B.L. designed and conceptualized the project; Z.Y.H., G.Q.C., G.P.L. and X.F.J. designed the experiments; X.F.J., G.P.L. and Z.Y.H. performed the experiments; X.F.J., Z.Y.H., G.Q.C. and C.J.Q. analyzed the data. X.F.J. wrote the manuscript and J.Q.C., Z.B.L. and G.P.L. contributed extensively in revising the manuscript. All authors have read and approved the final manuscript.

Ethics approval and consent to participate

This study has been approved by the Institutional Animal Care and Use Committee of the Zhejiang Sci-Tech University. Protocol no. 067714.

Consent for publication

Not applicable.

Declaration of competing interest

The authors declare that there is no conflict of interest regarding the publication of this paper.

Acknowledgments

We thank Dr. Zhong Liang for kindly providing the transgenosis zebrafish and reviewing the manuscript.

Appendix A. Supplementary data

Supplementary data to this article can be found online at https://doi.org/10.1016/j.fsi.2019.09.075.

References

[1] C.L. Chaffer, R.A. Weinberg, A perspective on cancer cell metastasis, Science 331 (6024) (2011) 1559–1564.
[2] L.R. Zarour, S. Anand, K.G. Billingsley, et al., Colorectal cancer liver metastasis:

evolving paradigms and future directions, Cmgh. Cell. Mol. Gastroenterol. Hepatol. 3 (2) (2017) 163–173.
[3] L. Sun, H. Hu, L. Peng, et al., P-cadherin promotes liver metastasis and is associated with poor prognosis in colon cancer, Am. J. Pathol. 179 (1) (2011) 380–390.
[4] A. Frilling, I.M. Modlin, M. Kidd, et al., Recommendations for management of patients with neuroendocrine liver metastases, Lancet Oncol. 15 (1) (2014) e8–e21.
[5] W. Maonan, Z. Jingzhou, Z. Lishen, et al., Role of tumor microenvironment in tumorigenesis, J. Cancer 8 (5) (2017) 761–773.
[6] J.H. Lee, S.W. Lee, The roles of carcinoembryonic antigen in liver metastasis and therapeutic approaches, Gastroenterol. Res. Pract. (13) (2017) 1–11 2017.
[7] I. Yoshiro, K. Kenji, I. Susumu, et al., The role of chemokines in promoting colorectal cancer invasion/metastasis, Int. J. Mol. Sci. 17 (5) (2016) 643.
[8] X.S. Cheng, Y.F. Li, J. Tan, et al., CCL20 and CXCL8 synergize to promote progression and poor survival outcome in patients with colorectal cancer by collaborative induction of the epithelial-mesenchymal transition, Cancer Lett. 348 (1–2) (2014) 77–87.
[9] J. Odenthal, R. Takes, P. Friedl, Plasticity of tumor cell invasion: governance by growth factors and cytokines, Carcinogenesis 37 (12) (2016) 1117–1128.
[10] Y.B. Zheng, H.P. Luo, Q. Shi, et al., miR-132 inhibits colorectal cancer invasion and metastasis via directly targeting ZEB2, World J. Gastroenterol. 20 (21) (2014) 6515–6522.
[11] S.R. Woo, M. Fuertes, L. Corrales, et al., STING-dependent cytosolic DNA sensing mediates innate immune recognition of immunogenic tumors, Immunity 41 (5) (2014) 830–842.
[12] L.F. Deng, H. Liang, M. Xu, et al., STING-dependent cytosolic DNA sensing promotes radiation-induced type I interferon-dependent antitumor immunity in immunogenic tumors, Immunity 41 (5) (2014) 843–852.
[13] Z. Wang, E. Celis, STING activator cGAMP enhances the anti-tumor effects of peptide vaccines in melanoma-bearing zebrafish, Cancer Immunol. Immunother. 64 (8) (2015) 1057–1066.
[14] S.K. Gupta, P.K. Yadav, A.K. Tiwari, et al., Poly (I:C) enhances the anti-tumor activity of canine parvovirus NS1 protein by inducing a potent anti-tumor immune response, Tumor Biol. 37 (9) (2016) 12089–12102.
[15] L. Lau, E.E. Gray, R.L. Brunette, et al., DNA tumor virus oncogenes antagonize the cGAS-STING DNA-sensing pathway, Science 350 (6260) (2015) 568–571.
[16] X. Cai, Y.H. Chiu, Z.J. Chen, The cGAS-cGAMP-STING pathway of cytosolic DNA sensing and signaling, Mol. Cell 54 (2) (2014) 289–296.
[17] H. Helen, D. Bikash, N. Nouri, Role of the CXCL8-CXCR1/2 Axis in cancer and inflammatory diseases, Theranostics 7 (6) (2017) 1543–1588.
[18] A. Kumar, M. Cherukumilli, S.H. Mahmoudpour, et al., ShRNA-mediated knockdown of, CXCL8, inhibits tumor growth in colorectal liver metastasis, Biochem. Biophys. Res. Commun. 500 (3) (2018) 731–737.
[19] A.E. Koch, P.J. Polverini, S.L. Kunkel, et al., Interleukin-8 as a macrophage-derived mediator of angiogenesis, Science 258 (5089) (1992) 1798–1801.
[20] Y. Liu, Y. Zhang, S. Wang, et al., Prospero-related homeobox 1 drives angiogenesis of hepatocellular carcinoma through selectively activating IL-8 expression, Hepatology 66 (6) (2017) 1894–1909.
[21] P. Andorfer, A. Heuwieser, A. Heinzel, et al., Vascular endothelial growth factor A as predictive marker for mTOR inhibition in relapsing high-grade serous ovarian cancer, BMC Syst. Biol. 10 (1) (2016) 33, https://doi.org/10.1186/s12918-016-0278-z.
[22] T.J. Goodwin, L. Huang, Investigation of phosphorylated adjuvants co-encapsulated with a model cancer peptide antigen for the treatment of colorectal cancer and liver metastasis, Vaccine 35 (19) (2017) 2550–2557.
[23] J. Go Dzik-Spychalska, K. Szyszka-Barth, Spychalski, et al., c-MET inhibitors in the treatment of lung cancer, Curr. Treat. Options Oncol. 15 (4) (2014) 670–682.
[24] A. Jahangiri, A. Nguyen, A. Chandra, et al., Cross-activating c-Met/β1 integrin complex drives metastasis and invasive resistance in cancer, Proc. Natl. Acad. Sci. U.S.A. 114 (41) (2017) 201701821.
[25] L.M.J. Lee, E.A. Seftor, G. Bonde, et al., The fate of human malignant melanoma cells transplanted into zebrafish embryos: assessment of migration and cell division in the absence of tumor formation, Dev. Dynam. 233 (4) (2005) 1560–1570.
[26] C. Santoriello, L.I. Zon, Hooked! Modeling human disease in zebrafish, J. Clin. Investig. 122 (7) (2012) 2337–2343.
[27] X.Y. Zhu, B. Xia, H.C. Liu, et al., Closantel suppresses angiogenesis and cancer growth in zebrafish models, Assay Drug Dev. Technol. 14 (5) (2016) 282–290.
[28] R.S. Kerbel, Tumor angiogenesis, N. Engl. J. Med. 358 (19) (2008) 2039–2049.
[29] X.F. Jiang, Z.F. Liu, A.F. Lin, et al., Coordination of bactericidal and iron regulatory functions of hepcidin in innate antimicrobial immunity in a zebrafish model, Sci. Rep. 7 (1) (2017) 4265–4271.